

## EFFECT OF RADIATION DEFECTS ON THE ELECTRONIC STRUCTURE OF ZIRCON BY X-RAY PHOTOELECTRON SPECTROSCOPY DATA

Yu. V. Shchapova,<sup>1</sup> S. L. Votyakov,<sup>1</sup> M. V. Kuznetsov,<sup>2</sup>  
and A. L. Ivanovskii<sup>2</sup>

UDC 541.16

X-Ray photoelectron spectroscopy (XPS) is used to study the electronic structure of radiation damaged samples of ZrSiO<sub>4</sub> zircon mineral at early and middle stages of its radiation destruction. The effects of radiation induced atomic disordering are found to be most distinctly manifested in the spectra of O1s states and to a smaller extent in the spectra of Si2p states, and also in the zircon valence band. Based on the quantum chemical calculation results the conclusion is drawn that the observed changes in XPS lines are caused by the formation of oxygen vacancy defects and an increase in the covalency of interatomic bonds near oxygen vacancies. For zircon samples with a low/moderate degree of radiation damage these changes reflect the initial stage of the polymerization of the ZrSiO<sub>4</sub> structure due to the formation of Si–O–Si chain fragments.

**Keywords:** zircon mineral, radiation defects, electronic structure, XPS.

### INTRODUCTION

Radiation disordering (the so-called radiation metamictization) of the zircon structure (ZrSiO<sub>4</sub>) due to  $\alpha$  decay of U and Th radioactive impurities in natural samples and of Pu in synthetic ceramics proposed for immobilization of radioactive wastes has recently been receiving much attention from researchers. It is important for the correct allowance for the degree of closeness of the U, Th/Pb subsystem in geochronological schemes and for the predictions of long-term stability of zircon waste forms with highly active radionuclides.

According to the current knowledge [1, 2], radiation destruction of zircon is determined by two main processes: 1) the formation of cascades of atomic displacements due to the ~30-40 nm paths of recoil daughter nuclei with the energy of about 70 keV, which appear in  $\alpha$  decay processes of radioactive elements ( $^{238}\text{U} \rightarrow ^{206}\text{Pb}$ ,  $^{235}\text{U} \rightarrow ^{207}\text{Pb}$ , and  $^{232}\text{Th} \rightarrow ^{208}\text{Pb}$ ); and 2) the formation of point defects because of the impact of  $\alpha$ -particles with the energy of about 5 MeV and a path length of ~10-20  $\mu\text{m}$ . Heavy recoil nuclei are responsible for the formation of localized amorphous regions with a small size and the structure sharply different from that of crystalline zircon, whereas  $\alpha$  particles are responsible for the formation of point defects in the crystal structure retaining the main features of ZrSiO<sub>4</sub>. Here the main type of defects are the Frenkel defects (vacancy — interstitial atom pairs) or, in the case of diffusion of interstitial atoms to the crystal surface, the Schottky defects (vacancies of O (mostly), Zr, and Si atoms). One may expect that at the early stages of radiation damage, when the

---

<sup>1</sup>A. N. Zavaritskii Institute of Geology and Geochemistry, Ural Division, Russian Academy of Sciences, Ekaterinburg. <sup>2</sup>Institute of Solid State Chemistry, Ural Division, Russian Academy of Sciences, Ekaterinburg; kuznetsov@ihim.uran.ru; ivanovskii@ihim.uran.ru. Translated from *Zhurnal Strukturnoi Khimii*, Vol. 51, No. 4, pp. 687-692, July-August, 2010. Original article submitted August 11, 2009.

**TABLE 1.** Characteristics of the Degree of Radiation Damage of Zircon Samples: Lattice Constants  $a$ ,  $c$  (according to X-ray diffraction\*) and the Normalized Volume Swelling ( $\Delta V^{**}$ ); Raman Shift  $\nu$  and Width  $\Delta\nu$  of the Peak of Asymmetric Stretching Vibrations of the  $\text{SiO}_4$  Tetrahedron (According to Raman Spectroscopy\*\*\*); Estimation Values of Effective  $\alpha$ -Radiation Doses  $D$

Sample	Lattice constant		$\Delta V$ , %	Raman spectral parameters		$D$ , $\alpha$ -particle/g
	$a$ , Å	$c$ , Å		$\nu$ , $\text{cm}^{-1}$	$\Delta\nu$ , $\text{cm}^{-1}$	
Z1	6.6000 ( $\pm 0.0005$ )	5.974 ( $\pm 0.001$ )	0.2	1009.6	5.4	$< 0.5 \cdot 10^{18}$
Z2	6.618 ( $\pm 0.003$ )	6.009 ( $\pm 0.005$ )	1.3	998.9	13.9	$\sim (1-2) \cdot 10^{18}$
Z3	6.614 ( $\pm 0.004$ )	6.02 ( $\pm 0.01$ )	1.2			

\*Measurements were performed by O. L. Galakhova on a DRON-3 X-ray diffractometer; lattice constants were determined by seven reflections ((321), (312), (400), (411), (420), (332), (204)) in the angular range  $2\theta = 50-70^\circ$ ;

\*\*Normalized volume swelling was estimated with respect to highly crystalline zircon of limburgites (Blagodat') with lattice constants  $a = 6.5952$  Å and  $c = 5.972$  Å.

\*\*\* Measurements were performed by É. G. Vovkotrub on a Renishaw inVia Reflex Raman microprobe with He-Ne laser excitation (633 nm) and a laser spot diameter of 1  $\mu\text{m}$  in the Institute of High Temperature Electrochemistry, Ural Division, Russian Academy of Sciences.

amorphous phase fraction is small, and also for chemically heterogeneous zircon crystals (namely, for regions with a low concentration of radioactive impurities adjacent to the regions with high concentrations),  $\alpha$  particles play the most active role in radiation destruction.

The purpose of the work is to study the effect of atomic disordering on the features of the electronic structure of zircon mineral at the early and middle stages of radiation destruction by X-ray photoelectron spectroscopy (XPS).

## EXPERIMENTAL

We studied the samples of natural zircon characterized by a different degree of radiation damage: Z1 are macroscopic single crystals from the Mir kimberlite pipe (Yakutia); Z2 are microcrystals from granitoids of the Berdyaush massif (Ural); Z3 are microcrystals from granulites of the Sokolovsk massif (Ural). Table 1 presents their characteristics. The degree of structural disordering and self-radiation dose ( $D$ ) of samples were estimated by comparing X-ray diffraction and Raman spectroscopy data based on the known relations between lattice constants, Raman shift and the width of the peak of asymmetric stretching vibrations of  $\text{SiO}_4$ , and the effective absorbed dose [3, 4]. The estimations yield the value  $D < 0.5 \cdot 10^{18}$   $\alpha$ -decays/g for sample Z1 and  $D \sim (1-2) \cdot 10^{18}$   $\alpha$ -decays/g for samples Z2 and Z3. Thus, sample Z1 is highly crystalline zircon (probably containing point structural defects), whereas samples Z2 and Z3 are zircons with a low/moderate degree of radiation damage, for which, according to [3], the amorphous phase fraction does not exceed 10-15%.

Since the XPS method analyzes a thin ( $\leq 5$  nm) surface layer of samples [5], then the surface preparation quality is of special importance for the validity of results and conclusions obtained for surface layers for the crystal bulk. For sample Z1 we analyzed the polished surface that was treated with a diamond file in air or with a diamond scraper in a vacuum chamber of the spectrometer directly before measurements (no differences were found in the spectra of surfaces treated in these two ways). For samples of Z2 and Z3 microcrystals we analyzed powder samples pressed into a substrate of metallic indium.

XPS studies were performed on an ESCALAB MK-II spectrometer; the  $\text{AlK}_{\alpha_{1,2}}$  ( $E = 1486.6$  eV) line was used for excitation; binding energies were calibrated by the  $\text{Au}4f_{7/2}$  (84.0 eV) line; a measurement error of the binding energy was 0.1 eV; spectral resolution was  $\sim 0.8-0.9$  eV. A sample charge correction was introduced with reference to carbon 1s energy (284.5 eV).

## RESULTS AND DISCUSSION

Fig. 1 shows the survey XP spectrum of zircon. Core level electrons form intense peaks:  $O1s$  in the 530-540 eV region;  $Zr3p_{3/2,3p_{1/2}}$  in the 335-355 eV region;  $Zr3d_{5/2,3d_{3/2}}$  in the 170-195 eV region;  $Si2s$  in the 155-165 eV region, and  $Si2p_{3/2,2p_{1/2}}$  (unresolved structure) in the 95-110 eV region. Moreover, in the figure, the  $C1s$  spectrum of surface carbon is seen (285-290 eV).

Table 2 presents the characteristics of core levels of the studied samples. In the transition from a highly crystalline sample (Z1) to samples with a moderate degree of radiation damage (Z2, Z3) the position of the  $O1s$  line maximum shifts by  $\sim 0.4$  eV to the high energy region, and its width increases by  $\sim 0.8$  eV. A similar but less pronounced effect (shift by 0.1-0.4 eV and broadening by  $\sim 0.5$  eV) is observed for the  $Si2p$  line. On the contrary, the energy and width of the  $Zr3d$  peak turns out to be almost insensitive to disordering of samples.

The energy of the  $O1s$  level in oxides is known to depend on the effective charge of oxygen and the degree of covalence of the bond between oxygen and cations of the nearest environment [5]. Therefore the shape and position of the  $O1s$  line were analyzed in detail for various degrees of sample disordering. From Fig. 2 it is seen that in the studied zircon samples the  $O1s$  band can be represented as a superposition of two components corresponding to two types of inequivalent oxygen atoms  $O_1$  and  $O_2$  with the binding energies of 531.0 eV and 532.3 eV (to approximate the spectrum we used the individual components in the Voigt form).

The energy of the  $O_1s$  level is close to the energy of the oxygen  $1s$  line in synthetic zircon and can be assigned to regular atoms of three-coordinated oxygen  $-\overset{\text{Zr}}{\underset{\text{Zr}}{\text{Si}}}-\text{O}$  in the crystal structure of  $ZrSiO_4$ . The  $O_2s$  level is shifted towards high energies and is close to the energy of the  $O1s$  level in quartz. In highly crystalline sample Z1, the relative concentration of  $O_2$

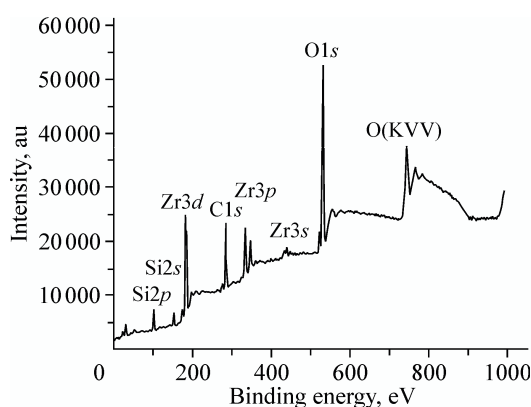
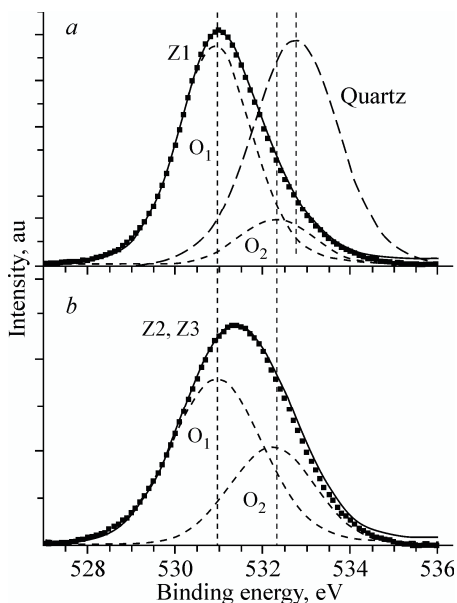


Fig. 1. Survey XP spectrum of zircon.

**TABLE 2.** Positions of Maxima and Bandwidths of Oxygen, Silicon, and Zirconium Core Levels in Zircon Samples with a Different Degree of Radiation Damage (Z1–Z3), and also in Synthetic Zircon  $ZrSiO_4$ , Quartz  $SiO_2$ , and Baddeleyite  $ZrO_2$  by the Data [8]

Sample	Binding energy/bandwidth, eV			Sample	Binding energy/bandwidth, eV		
	$O1s$	$Si2p$	$Zr3d$		$O1s$	$Si2p$	$Zr3d$
Z1*	530.1/2.1	101.5/1.8	182.7/1.8	$ZrSiO_4$	531.3/2.3	101.8/2.0	183.0/1.8
Z2	531.4/2.9	101.9/2.3	182.8/2.0	$SiO_2$	532.7/2.0	103.2/2.0	—
Z3	531.4/2.8	101.6/2.4	182.4/1.9	$ZrO_2$	530.0/1.4	—	181.9/1.4

\*Z1–Z3 are zircon samples with a different degree of radiation damage, see Table 1.



**Fig. 2.** O1s spectra of highly crystalline (Z1) and radiation disordered samples (Z2, Z3) of zircon and their decomposition into individual O<sub>1</sub> and O<sub>2</sub> components in the Voigt form. The O1s spectrum of quartz is also given, according to [8].

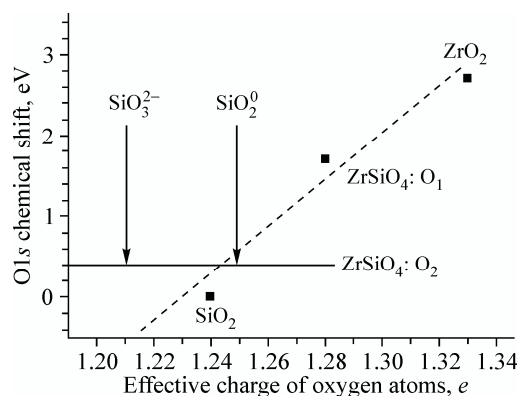


**Fig. 3.** Comparison of the chemical shift of O1s levels in zircon, quartz, and baddeleyite by the XPS data (for quartz and baddeleyite, according to [8]) with effective charges of oxygen atoms from quantum chemical calculations [6]. The O1s chemical shift in quartz is taken to be zero. Solid line denotes the O<sub>2</sub>1s chemical shift in zircon; arrows denote the calculated values of effective charges on oxygen atoms near vacancy defects in zircon [7].

atoms is  $O_2/O_1 = 0.2$ ; in radiation damaged samples Z2 and Z3, the relative concentration of O<sub>2</sub> atoms substantially increases ( $O_2/O_1 = 0.6$ ).

In order to understand the nature of O<sub>2</sub> atoms, we used the results of our quantum chemical calculations of effective charges of oxygen atoms in an ideal zircon crystal [6] and in zircon containing typical radiation point defects [7]: vacancies and divacancies of oxygen atoms (SiO<sub>3</sub><sup>2-</sup> and SiO<sub>2</sub><sup>0</sup> groups respectively). Fig. 3 shows a comparison between the experimental values of the chemical shift of O1s levels in zircon, quartz, and baddeleyite by the XPS data (for quartz and baddeleyite — according to the data [8]) and the effective charges of oxygen atoms calculated in [6, 7] for the mentioned defect-free crystals and also for zircon containing oxygen vacancy defects. In the latter case, the averaged values of effective charges on oxygen atoms of defect SiO<sub>3</sub><sup>2-</sup> and SiO<sub>2</sub><sup>0</sup> groups are given. Based on the data for crystalline zircon, quartz, and baddeleyite, we obtained a linear dependence of the effective charge on the chemical shift. In defect regions of SiO<sub>3</sub><sup>2-</sup> and SiO<sub>2</sub><sup>0</sup>, oxygen atoms are characterized by a more covalent type of chemical bonding with silicon atoms and lower effective charges than oxygen atoms of regular SiO<sub>4</sub><sup>4-</sup> tetrahedra; the values of their effective charges (shown by arrows in Fig. 3) are close in value to the charge of oxygen atoms in quartz. At high concentrations of vacancy defects oxygen atoms of the specified type can be expected to be revealed by XPS in the form of a separate high-energy component (component with a small chemical shift with respect to quartz).

Based on the above, we assigned the O<sub>2</sub>1s band with the energy of 532.30 eV observed by XPS to oxygen atoms of defect SiO<sub>3</sub><sup>2-</sup> and SiO<sub>2</sub><sup>0</sup> groups. An increase in the intensity of this band with increasing degree of radiation damage of zircon is well consistent with the interpretation.

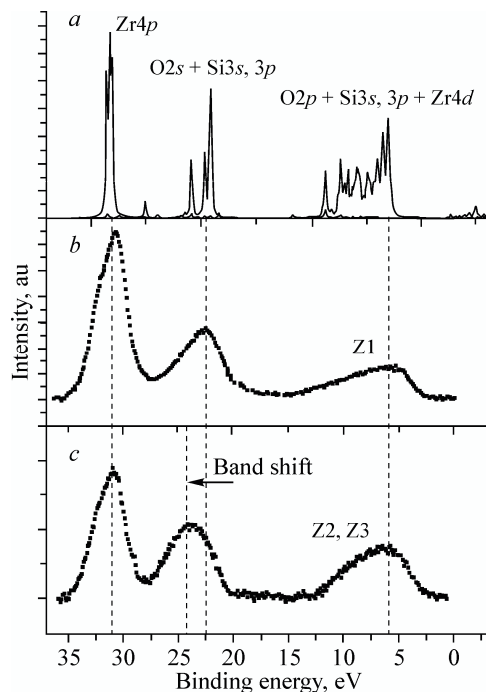


**Fig. 4.** Calculated [6] (a) and experimental (b, c) XP spectra of the valence band of highly crystalline (a, b) and radiation disordered (c) zircon.

Note that the work [7] revealed the substantial relaxation of the zircon structure during the formation of  $\text{SiO}_3^{2-}$  and  $\text{SiO}_2^0$  point defects. In particular, it is shown that the neighboring  $\text{SiO}_4$  tetrahedra shift towards the defect tetrahedra, which is accompanied by the formation of Si–O–Si bonds absent in the original structure of  $\text{ZrSiO}_4$ . The formation of oxygen-vacancy defects can be considered as the initial stage of the polymerization of silicon-oxygen tetrahedra, which is known for zircons with a high degree of radiation destruction [9, 10]. Therefore, the emergence of the  $\text{O}_21s$  band in samples with a low/moderate degree of radiation damage can be attributed to the formation of Si–O–Si chain fragments at the initial stage of the polymerization of the silicon-oxygen sublattice in zircon.

The direct information on the features of chemical bonding can be obtained by the analysis of the valence band of the crystal. Fig. 4 shows the calculated valence band spectrum of crystalline zircon [6] and experimental XPS valence band spectra for samples Z1, Z2, Z3. A comparison of the calculated and experimental spectra of highly crystalline zircon (Z1) indicates that the main features of the  $\text{ZrSiO}_4$  valence band are well reproduced in the calculations, thus confirming the correctness of simulation [6, 7] and also allowing the interpretation of the main bands of experimental spectra. It is seen that the upper part of the valence band is formed by  $2s, 2p$  states of oxygen atoms with an admixture of  $\text{Si}3s, 3p$  and  $\text{Zr}4d$  states. The  $\text{O}2s$  and  $\text{O}2p$  bandwidths are 1.8 eV and 6.0 eV respectively; the total bandwidth of oxygen states is  $\Delta E = 18.1$  eV. The  $\text{Zr}4p$  states form narrow peaks deep in the valence band; their energy is by 6.5 eV higher than the energy of the  $\text{O}2s$  band maximum.

The main feature of the valence band spectra of radiation disordered samples (Z2 and Z3), as compared to those of the highly crystalline sample (Z1), is a  $\sim 2$  eV shift of the  $\text{O}2s$  band to the high energy region. This experimental result well corresponds to the calculation data predicting an increase in the energy range of the  $2s$  and  $2p$  states of oxygen due to an increase in the covalence of chemical bonding in the defect regions of zircon [7] and also highly polymerized (framework) structure of quartz [11]. Note that a similar pattern (broadening of the energy states of oxygen in the transition from a

structure with three-coordinated oxygen to a structure with two-coordinated (bridging) oxygen) we also have previously observed in glassy phosphates [12].

Thus, a change in the electronic structure and characteristics of chemical bonding in radiation damaged samples can be revealed in the XP valence band spectra of zircon by the broadening of the band of its oxygen states.

## CONCLUSIONS

X-ray photoelectron spectroscopy is used to study the electronic structure of radiation damaged samples of zircon mineral with a low/moderate degree of radiation destruction. The effects of radiation induced atomic disordering are found to be most noticeable in the spectra of core O1s states and to a lesser extent in the spectra of core Si2p states and also in the valence band of zircon. Based on the results of quantum chemical calculations, the conclusion is made that changes in the spectral characteristics are caused by the formation of oxygen vacancy defects and an increase in the covalency of interatomic bonds near oxygen vacancies. For zircon samples with a low/moderate degree of radiation damage these changes reflect the initial polymerization stage of the structure due to the formation of Si–O–Si chain fragments.

The authors are grateful to A. A. Krasnobaev for the provided samples of zircons.

The work was supported by Programs Nos. 14 and 20 of the Presidium of the Russian Academy of Sciences, by the Interdisciplinary Integration Program of the Ural Division of the Russian Academy of Sciences, and RFBR projects Nos. 07-05-00097a and 09-05-00513a.

## REFERENCES

1. W. J. Weber, *Nuclear Instruments Methods Phys. Res. Sec. B*, **166/167**, 98-106 (2000).
2. R. C. Ewing, A. Meldrum, L. Wang, et al., in: *Zircon. Reviews in Mineralogy and Geochemistry*, J. M. Hanchar and P. W. O. Hoskin (eds.), **53**, 387-425 (2003).
3. S. Rios, E. K. H. Salje, M. Zhang, and R. C. Ewing, *J. Phys.: Condens. Matter.*, **12**, 2401-2412 (2000).
4. C. S. Palenik, L. Nasdala, and R. C. Ewing, *Am. Miner.*, **88**, 770-781 (2003).
5. K. Siegbahn, C. Nordling, A. Fahlman, et al, *ESCA-Atomic, Molecular and Solid State Structure by Means of Electron Spectroscopy, Nova Acta Regiae Soc. Sci. Upsaliensis*, Upsala, Sweden (1967).
6. Yu. V. Shchapova and S. L. Votyakov, *Geology of the Ural and Adjacent Territories* [in Russian], Izd. UrO RAN, Ekaterinburg (2007), pp. 285-309.
7. Yu. V. Shchapova, D. A. Zamyatin, and S. L. Votyakov, in: *Structure and Diversity of the Mineral World* [in Russian], Intern. Workshop Proc., Syktyvkar (2008), pp. 51-53.
8. M. J. Guittet, J. P. Crocombette, and M. Gautier-Soyer, *Phys. Rev.*, **B63**, No. 12, art. 125117 (2001).
9. I. Farnan, *Phase Transit.*, **69**, 47-60 (1999).
10. I. Farnan and E. K. H. Salje, *J. Appl. Phys.*, **89**, 2084-2090 (2001).
11. Yu. V. Shchapova, S. L. Votyakov, and A. L. Ivanovskii, *IGG UrO RAN Annual*, 2003 [in Russian], Izd. UrO RAN, Ekaterinburg (2004), pp. 296-406.
12. A. F. Zatsepin, V. S. Kortov, and Yu. V. Shchapova, *Fiz. Tverd. Tela*, **39**, 1366-1372 (1997).